

Locating of Multi-phase Faults of Ungrounded Distribution System

Dubey, A.; Sun, H.; Nikovski, D.; Zhang, J.; Takano, T.; Ohno, T.

TR2014-100 October 2014

Abstract

This paper proposes a new method for locating multi-phase faults in ungrounded distribution systems, including phase-to-phase faults, double-phase-to-ground faults, and three-phase faults. Through identification of the faulty feeder section, the fault location algorithm is only implemented on the faulty section of the feeder, thus avoiding the unnecessary computations. A two-ended fault location algorithm is implemented for both two and three phase faults on the mainline of the faulty section. Two different one-ended fault location algorithms are also implemented for handling two-phase faults and three-phase faults on the laterals of the faulty section respectively. The proposed fault location algorithms make no assumption regarding the fault impedance, thus estimation of fault location is invariant to fault impedances. Numerical examples are given to demonstrate the effectiveness of the proposed method.

IEEE PowerCon 2014

This work may not be copied or reproduced in whole or in part for any commercial purpose. Permission to copy in whole or in part without payment of fee is granted for nonprofit educational and research purposes provided that all such whole or partial copies include the following: a notice that such copying is by permission of Mitsubishi Electric Research Laboratories, Inc.; an acknowledgment of the authors and individual contributions to the work; and all applicable portions of the copyright notice. Copying, reproduction, or republishing for any other purpose shall require a license with payment of fee to Mitsubishi Electric Research Laboratories, Inc. All rights reserved.

Locating of Multi-phase Faults of Ungrounded Distribution System

Anamika Dubey, *Student Member, IEEE*, Hongbo Sun, *Senior Member, IEEE*, Daniel Nikovski, *Member, IEEE*, Jinyun Zhang, *Fellow, IEEE*, Tomihiro Takano, Yasuhiro Kojima, *Member, IEEE* and Tetsufumi Ohno

Abstract— This paper proposes a new method for locating multi-phase faults in ungrounded distribution systems, including phase-to-phase faults, double-phase-to-ground faults, and three-phase faults. Through identification of the faulty feeder section, the fault location algorithm is only implemented on the faulty section of the feeder, thus avoiding the unnecessary computations. A two-ended fault location algorithm is implemented for both two and three phase faults on the mainline of the faulty section. Two different one-ended fault location algorithms are also implemented for handling two-phase faults and three-phase faults on the laterals of the faulty section respectively. The proposed fault location algorithms make no assumption regarding the fault impedance, thus estimation of fault location is invariant to fault impedances. Numerical examples are given to demonstrate the effectiveness of the proposed method.

Index Terms— Fault location analysis; multi-phase fault; ungrounded distribution systems

I. INTRODUCTION

DISTRIBUTION systems are susceptible to various short circuit faults. The faults need to be cleared as soon as possible to reduce power outage time and avoid equipment damage. The clearing of faults requires an accurate and fast estimation of locations of the faults.

Many fault location algorithms have been proposed for distribution systems, including impedance-based methods [1-6], traveling waves based methods [7-10], and knowledge-based methods [11-12]. Amongst all methods proposed in the literature, impedance-based fault location methods are most generic, practical and straightforward to implement [1-2]. Unlike traveling waves based methods, no additional equipment, such as the GPS system, fault transient

detectors are required [10]. Also, impedance-based methods require no training sets, thus are more generic in their approach. A two stage fault location algorithm using both pre-fault and fault voltage and current measurements was proposed in [5]. The method does not made any assumption regarding the line impedances and load taps, thus it is reasonably accurate even in a heavily taped feeder system. An extended fault-location formulation for a general distribution system was proposed in [6]. The method is based on apparent fault impedance calculation and can calculate sufficiently accurate fault location in a distribution system with intermediate taps, lateral and with heterogeneous lines. Although promising, the impedance-based fault location algorithms developed so far still have their own limitations. These algorithms address mostly single-phase to ground faults and are applicable to only resistance faults; therefore they result in significant errors in case of impedance fault. Also, these are iterative algorithms and scan the entire distribution feeder to locate the fault, thus doing unnecessary computations.

This paper proposes a novel method for determining the locations of multi-phase faults in an ungrounded distribution system based on the fundamental frequency measurements collected from the feeder breakers at the substation and the intelligent switches along the feeders. The proposed method first identifies the faulty feeder section, and then according to the location of fault line, the fault location is determined through detailed circuit and topology analysis of the faulty section. Both one-ended, and two-ended fault location algorithms are proposed to handle feeder sections with different measuring and topology conditions. A two-ended fault location algorithm is proposed for locating two and three phase faults on the mainline of the faulty section. Two different one-ended fault location algorithms are also proposed for locating two-phase faults and three-phase faults on the laterals of the faulty section respectively. The proposed fault location algorithms make no assumption regarding the fault impedance, thus can be applied to both bolted faults and impedance faults. Numerical examples are given to demonstrate the effectiveness of the proposed method.

Manuscript submitted July 10, 2014.

Anamika Dubey is with the University of Texas at Austin, Austin, Texas 78712 USA.

Hongbo Sun, Daniel Nikovski and Jinyun Zhang are with the Mitsubishi Electric Research Laboratories, Cambridge, MA 02139 USA.

Tomihiro Takano, Yasuhiro Kojima and Tetsufumi Ohno are with the Mitsubishi Electric Corporation, Hyogo 661-8661 Japan.

II. DETERMINING FAULT TYPE AND FAULTED FEEDER SECTION OF UNGROUNDED SYSTEMS

A. Ungrounded Distribution Systems with Advanced Protection Scheme

Fig. 1 shows an example of ungrounded distribution system with advanced protection scheme. It includes a distribution substation in which a three-phase transformer receives electric power from power transmission systems, and provides the power to downstream feeders. The windings of the transformer are ungrounded and can use either WYE or DELTA connections. In Fig. 1, the primary winding of the transformer uses the DELTA connection, and secondary winding uses the WYE connection. The feeder transfers powers to the loads through three-phase three-wire lines, and all loads can be DELTA connected. The distribution systems operate in a radial configuration.

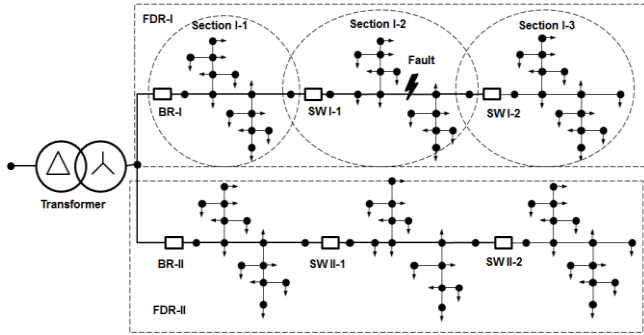


Fig. 1. An example of ungrounded distribution system with advanced protection scheme

Each feeder can have one feeder breaker located at the substation, and several intelligent switches along the feeder. The breakers and switches are both equipped with sensor units that can provide synchronized three-phase voltage and three-phase current measurements. According to the location of switches, each feeder can be partitioned into several sections. In Fig. 1, the system has two feeders, FDR-I, and FDR-II. Feeder FDR-1 includes one feeder breaker, BR-I, two switches SWI-1 and SWI-2, and three feeder sections I-1, I-2 and I-3.

Based on the number of switchable devices at the boundaries of a feeder section, a feeder section can be called as a one-ended section, or two-ended section. A one-ended section is defined as a feeder section that only has a feeder breaker or intelligent switch at its upstream boundary. A two-ended section is a feeder sections that has one circuit breaker, or intelligent switch at its upstream boundary, and one intelligent switch at its downstream boundary. A one-ended feeder section can also be treated as a lateral. In Fig. 1, section I-1, and section I-2 are two-ended feeder sections, and section I-3 is a one-ended feeder section.

B. Determining the Fault Type and Faulted Feeder Section

The type of the fault is determined based on the measured voltages and currents at fundamental frequency on the feeder breakers taken during the fault.

The measured currents on any feeder breaker are first checked to see whether there is over-current existing on any phases of the breaker. If there is no over-current, then there is no multiple-phase fault downstream to the feeder breaker.

If there are over-currents on the breaker, then there is a double or three phase fault occurring in the system. The fault type is determined according to the number of phases with over-currents. If there are two phases having over-currents, then the fault is either a double phase to ground fault, or a phase-to-phase fault, and the actual type is further determined by checking whether there is over-voltage on the phase without over-current. If there is over-voltage existing, then the fault type is a double-phase-to-ground fault. Otherwise, the type of the fault is a phase-to-phase fault. If there are three phases having over-currents, then there is a three phase fault downstream to the feeder breaker.

A phase x is determined as having over-current, when the following condition is met:

$$|I_{p,x}|/I_{p,x}^{rated} \geq \bar{I} \quad x \in \{a, b, c\} \quad (1)$$

where, $|I_{p,x}|$ and $I_{p,x}^{rated}$ are the magnitude of measured current, and rated normal current at the switch p on phase x , \bar{I} is the threshold of current ratio of measured current over rated normal current used for over current status determination. For example, \bar{I} can be set as 3.0.

A phase x is determined as having over-voltage, if the following condition is met:

$$|V_{p,x}| \geq \bar{V} \quad x \in \{a, b, c\} \quad (2)$$

where, $|V_{p,x}|$ is the magnitude of voltage measured at switch p on the phase x , and \bar{V} is the threshold of voltage magnitude used for over voltage status determination. For example, \bar{V} can be set as 1.40 per unit

A feeder is determined as a faulty one, if there are over-currents on its breaker. The phases that have over-currents are the faulty phases.

A faulted feeder section is the farthest section from the root of the faulty feeder that has over-currents on its upstream switch.

III. IDENTIFICATION OF THE FAULTED LINE TYPE

For a faulted two-ended feeder section, the faulty line segment can be either at the mainline of the section, i.e., the shortest path between two switches, or at the laterals of the section, i.e., the portion of feeder section started at the bus on the mainline.

The type of faulted line is identified based on the estimation of the fault voltages at each bus along the mainline using the measurements obtained from the two switches.

The voltage and current measured at the upstream switch is used to determine the first set of the voltages and currents at each bus along the mainline of the faulted section using three-phase circuit analysis.

Similarly, the voltage and current measured at the downstream switch is used to determine the second set of fault voltages and currents at each bus of the faulted section.

Both set of voltages are compared to identify the type of faulty line.

A. Calculating the fault voltages and currents using measurements at the upstream switch

Fig. 2 and 3 shows two examples for calculating voltage and current of a two-ended feeder section.

Let, $V_{f,A}^k, I_{f,A}^k$ be the vectors of voltages and currents measured at the upstream switch, switch A during the fault. While calculating voltages and currents at bus $(k+1)$ two cases can arise. One case is that bus $(k+1)$ is not connected to a lateral as shown in Fig.2, and the other is bus $(k+1)$ is connected to a lateral as shown in Fig. 3.

If bus $(k+1)$ is not connected to a lateral as shown in Fig. 2, using the impedance matrix of line segment between bus k and $(k+1)$, Z_{li}^k , and load impedance matrix at bus $(k+1)$, Z_L^{k+1} , the vectors of voltages and currents at bus $(k+1)$ are determined according to:

$$V_{f,A}^{k+1} = V_{f,A}^k - Z_{li}^k I_{f,A}^k \quad (3)$$

$$I_{f,A}^{k+1} = I_{f,A}^k - (Z_L^{k+1})^{-1} V_{f,A}^{k+1} \quad (4)$$

where, $V_{f,A}^{k+1}$ and $I_{f,A}^{k+1}$ are the vectors of voltages at bus $(k+1)$ and currents flowing from bus $(k+1)$ to bus $(k+2)$ determined using the measurements at the upstream switch A.

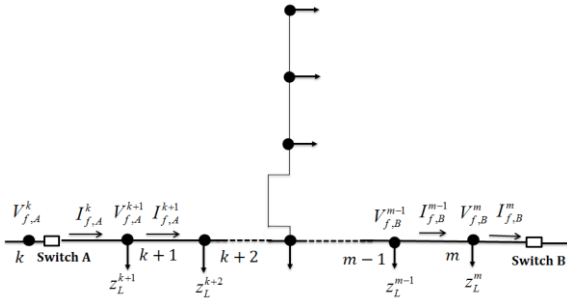


Fig. 2. A feeder section with no laterals connected to buses $(k+1)$ and $(m-1)$

If bus $(k+1)$ is connected to a lateral as shown in Fig. 3, the bus $(k+1)$ voltage calculation is same as the previous case. Hence, $V_{f,A}^{k+1}$ is given by (3). However to calculate the currents flowing in next line segment between bus $(k+1)$ and bus $(k+2)$, the currents flowing into the lateral fed by bus $(k+1)$, $I_{f,A}^{kl}$ is also determined.

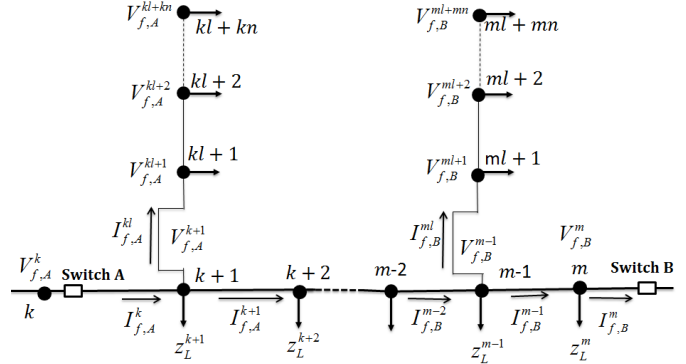


Fig. 3. A feeder section with laterals connected to buses $(k+1)$ and $(m-1)$

Thus, the vector of currents $I_{f,A}^{k+1}$ is given by (5):

$$I_{f,A}^{k+1} = I_{f,A}^k - (Z_L^{k+1})^{-1} V_{f,A}^{k+1} - I_{f,A}^{kl} \quad (5)$$

The current $I_{f,A}^{kl}$ can be determined based on the relationship between the bus injection currents and bus voltages of all the buses in the lateral. In the example of Fig. 3, the lateral fed by bus $(k+1)$ includes a set of buses, bus $(kl+1)$, bus $(kl+2)$, ..., and bus $(kl+kn)$.

The voltage and current relationship for the lateral fed by bus $(k+1)$ can be expressed as:

$$\begin{bmatrix} I_{f,A}^{kl} \\ 0 \\ \vdots \\ 0 \end{bmatrix} = Y_{l,k+1} \begin{bmatrix} V_{f,A}^{k+1} \\ V_{f,A}^{kl+1} \\ \vdots \\ V_{f,A}^{kl+kn} \end{bmatrix} \quad (6)$$

where, $Y_{l,k+1}$ is the bus admittance matrix determined based on the impedance of line segments and load impedances for the lateral connected to bus $(k+1)$. Only bus $(k+1)$ has current injections and all other buses do not have injected currents.

Regrouping the set of buses into two sets, one only includes bus $(k+1)$, and the other includes all buses except bus $(k+1)$, and the lateral admittance matrix $Y_{l,k+1}$ can also be partitioned as follows:

$$Y_{l,k+1} = \begin{bmatrix} Y_{l,k+1}^{11} & Y_{l,k+1}^{12} \\ Y_{l,k+1}^{21} & Y_{l,k+1}^{22} \end{bmatrix} \quad (7)$$

where, $Y_{l,k+1}^{11}$ and $Y_{l,k+1}^{22}$ are the self-admittance matrices of the first and second set of buses, $Y_{l,k+1}^{12}$ and $Y_{l,k+1}^{21}$ are the mutual-admittance matrices between the first and second sets of buses respectively.

Based on Equations (6) and (7), the vector of currents on the lateral can be determined as:

$$I_{f,A}^{kl} = \left\{ Y_{l,k+1}^{11} - Y_{l,k+1}^{12} (Y_{l,k+1}^{22})^{-1} Y_{l,k+1}^{21} \right\} V_{f,A}^{k+1} \quad (8)$$

B. Calculating fault voltages and currents using measurements at the downstream switch

A similar set of calculations are repeated to obtain voltage and current at each bus using the measurements obtained from downstream switch, switch B.

Let, $V_{f,B}^m, I_{f,B}^m$ be the vectors of voltages and currents measured at the switch B during fault. Similar to the previous case, while calculating voltages and currents at bus $(m-1)$, two cases can arise.

If bus $(m-1)$ is not connected to a lateral as shown in Fig. 2, using the line impedance matrix between bus m and bus $(m-1)$, z_{ll}^{m-1} , and load impedance matrix at bus m , z_L^m , the voltages at bus $(m-1)$ and currents flowing out of bus $(m-1)$ is determined as:

$$I_{f,B}^{m-1} = I_{f,B}^m + (z_L^m)^{-1} V_{f,B}^m \quad (9)$$

$$V_{f,B}^{m-1} = V_{f,B}^m + z_{ll}^{m-1} I_{f,B}^{m-1} \quad (10)$$

where, $V_{f,B}^{m-1}$ and $I_{f,B}^{m-1}$ are the vectors of voltages at bus $(m-1)$ and currents flowing from bus $(m-1)$ to bus m determined using the measurements at the downstream switch, switch B.

If bus $(m-1)$ is connected to a lateral as shown in Fig. 3, $I_{f,B}^{m-1}$ and $V_{f,B}^{m-1}$ are determined using Equations (9) and (10). However, calculation of current flowing out of bus $(m-2)$, $I_{f,B}^{m-2}$, requires currents flowing in the lateral, $I_{f,B}^{ml}$. Current $I_{f,B}^{m-2}$ is given by

$$I_{f,B}^{m-2} = I_{f,B}^{m-1} + (z_L^{m-1})^{-1} V_{f,B}^{m-1} + I_{f,B}^{ml} \quad (11)$$

The current $I_{f,B}^{ml}$ can be determined using the same method as discussed for upstream switch measurement. Following the same procedure, the current $I_{f,B}^{ml}$ is determined by (12):

$$I_{f,B}^{ml} = \{Y_{l,m-1}^{11} - Y_{l,m-1}^{12} (Y_{l,m-1}^{22})^{-1} Y_{l,m-1}^{21}\} V_{f,B}^{m-1} \quad (12)$$

where, $Y_{l,m-1}^{11}$ and $Y_{l,m-1}^{22}$ are the self-admittance matrices of the first and second set of buses, $Y_{l,m-1}^{12}$ and $Y_{l,m-1}^{21}$ are the mutual-admittance matrices between the first and second sets of buses, and the first set of buses includes only bus $(m-1)$, and the second set of buses include all bus in the lateral except bus $(m-1)$.

The equations are recursively used to calculate voltages at each bus.

C. Determining the type of faulty line

Based on the voltage and current recorded at both upstream and downstream switches, the voltages at each bus along the mainline are determined. Thus, two sets of voltages are available at any bus n , $V_{f,A}^n$ and $V_{f,B}^n$.

Fig. 4 and Fig.5 show two example of the fault location.

If the fault is in the mainline, as shown in Fig.4, the voltages at any bus n , $V_{f,A}^n$ and $V_{f,B}^n$ corresponding to faulty phases will not be equal. Therefore, each bus along the mainline will satisfy (13) for a small threshold δ , for example, 0.0001.

$$\|V_{f,A}^n - V_{f,B}^n\| > \delta \quad (13)$$

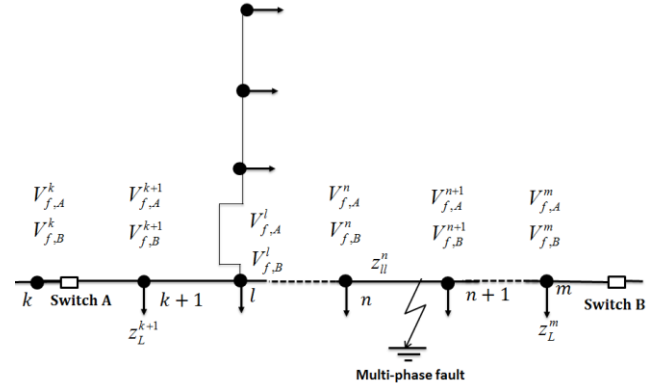


Fig. 4. A feeder section with a fault in the mainline

If the fault is at a bus or in the lateral connected to a bus, as shown in Fig. 5, the bus voltage at the bus l , determined during fault condition using both switch A and switch B measurements will satisfy (14) for a small threshold δ :

$$\|V_{f,A}^l - V_{f,B}^l\| < \delta \quad (14)$$

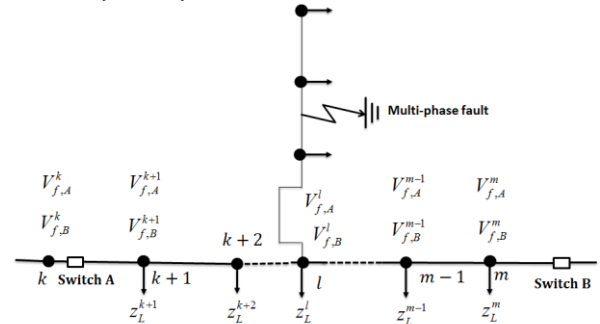


Fig. 5. A feeder section with a fault in the lateral

This condition implies that the voltages determined at the faulty bus or at the lateral connected to the faulty bus using the two measurements are approximately equal. If (14) is satisfied for bus l , then fault is either at bus l , or at the lateral connected to bus l .

IV. DETERMINING THE LOCATION OF FAULT

For the mainline of a two-ended feeder section, the voltage and current readings are available at both ends. For the laterals of a two-ended feeder section, or a one-ended feeder section, only one measurement is available. Therefore, based on available voltage and current measurements, both two-ended and one-ended algorithms are used.

A. Locating faults at the mainlines

Fig. 6 shows the fault is at the mainline and between buses n and $(n+1)$. Two sets of voltages and currents are available at both buses n and $(n+1)$. Let V_F be the voltage at the fault location. Then, using circuit analysis the following equations are obtained:

$$V_{f,A}^n = V_F + dz_{ll}^n I_{f,A}^n \quad (15)$$

$$V_{f,B}^n = V_F + dz_{ll}^n I_{f,B}^n \quad (16)$$

$$V_{f,A}^{n+1} = V_F - (1-d)z_{ll}^n I_{f,A}^n \quad (17)$$

$$V_{f,B}^{n+1} = V_F - (1-d)z_{ll}^n I_{f,B}^n \quad (18)$$

where, d is the ratio of distance from bus n to the fault location over the total length of the line segment between bus n and $(n+1)$, z_{ll}^n is the impedance of line segment between bus n and $(n+1)$.

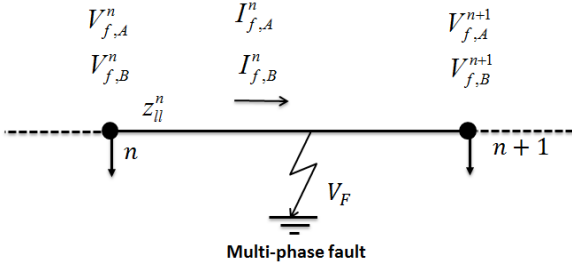


Fig. 6. A fault in the mainline and between buses n and $(n+1)$

Using (15)-(18), for the faulted line segment between bus n and $(n+1)$, the following relationship can be obtained:

$$\frac{V_{f,A}^{n+1} - V_{f,B}^{n+1}}{V_{f,A}^n - V_{f,B}^n} = -\frac{(1-d)}{d} \quad (19)$$

Accordingly, we can have:

$$\angle(V_{f,A}^{n+1} - V_{f,B}^{n+1}) - \angle(V_{f,A}^n - V_{f,B}^n) = \pi \quad (20)$$

According to (20), for a faulty line segment, the difference between angle differences of corresponding voltages in the first and the second set determined at the upstream and downstream buses is close to 180 degree.

Now, if any two adjacent buses, n and $(n+1)$ in the main feeder satisfy (20), then the fault is in the line segment between buses n and $(n+1)$. Once the faulted line segment is identified, (19) is used to calculate the ratio of distance to the fault over line length, d . Only the faulted phases are used for (19) and (20).

B. Locating faults at the laterals

If the fault is in one of the laterals, then the voltage determined using both measurements at the bus connected to the lateral, l for a two-ended section will be approximately equal:

$$V_{f,A}^l = V_{f,B}^l = V_f^l \quad (21)$$

Hence, in this case effectively we have only one measurement for the fault location calculation. Fig. 7 shows an example of a lateral having a fault.

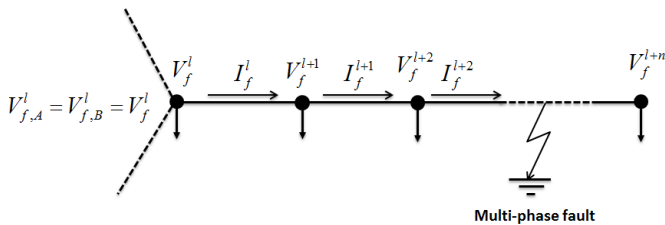


Fig. 7. A lateral having a fault

Two separate algorithms are proposed for a double-phase fault, and a three-phase fault. For a phase-to-phase fault or a double-phase-to-ground fault, the location of the fault is determined at a first point on an un-faulty phase of the lateral where a fault current equals an equivalent load current. For a three-phase fault, the location of the fault is determined at a point with a difference between imaginary parts of equivalent fault impedances at three phases below a threshold.

For any multi-phase fault, the following equations are used for determining fault voltage, current and impedance:

$$V_F = V_f^l - dz_{ll}^l I_f^l \quad (22)$$

$$I_F = I_f^l - I_L^l \quad (23)$$

$$Z_{F_{a,b,c}} = \frac{V_F}{I_F} \quad (24)$$

where, z_{ll}^l is the impedance of the line segment between buses l and $(l+1)$, V_F is the voltage at the fault location, I_F is the fault current at fault location, I_f^l is the faulted line current flowing in line segment, I_L^l is the load current flowing during the fault condition, $Z_{F_{a,b,c}}$ is the equivalent fault impedance at the fault location.

1). Algorithm for locating double-phase faults

Figs. 8 and 9 show examples of a double-phase-to-ground fault and a phase-to-phase fault at the line segment between buses l and $(l+1)$.

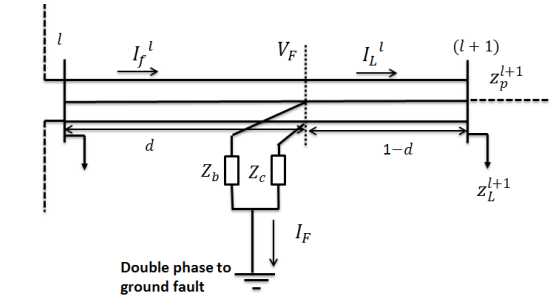


Fig. 8. A line segment with a double-phase-to-ground fault

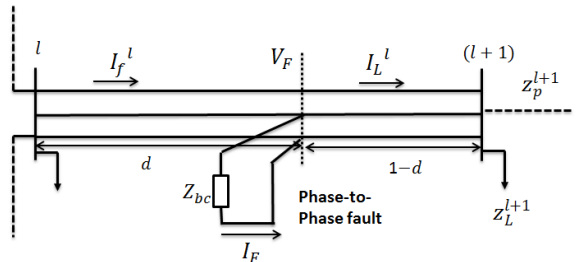


Fig. 9. A line segment with a phase-to-phase fault

For a double-phase fault, one of the phases is un-faulted. Let's assume phase b and c are the faulted phases, then phase a is the un-faulted phase. If the fault is at a location, f of line segment between bus l and bus $(l+1)$, the equivalent load current at phase a will be equal to fault current at phase a at the location:

$$I_L^{l(a)} = I_f^{l(a)} \quad (25)$$

While load currents at faulted phases, phase *b* and phase *c* can be determined using the following equation:

$$I_L^l = \frac{V_f^l - d z_{ll}^l I_f^l}{(1-d)z_{ll}^l + z_{eq}^{l+1}} \quad (26)$$

where, *d* is the ratio of distance from bus *l* to the fault location over the total length of the line segment between bus *l* and (*l* + 1); z_{eq}^{l+1} is the equivalent load impedance as seen by the line segment, and determined according to:

$$z_{eq}^{l+1} = \left[(z_p^{l+1})^{-1} + (z_L^{l+1})^{-1} \right]^{-1} \quad (27)$$

z_L^{l+1} is load impedance at bus (*l* + 1) and z_p^{l+1} is equivalent line and load impedance downstream bus (*l* + 1).

As shown in Fig. 7, since a lateral may contain many line segments with several load taps, the fault location is implemented sequentially for each line-segment. The load currents for each phase are determined along a line segment using (26) by varying the ratio of distance to fault over total length, *d*. The estimated fault location is obtained when the value of *d*, for which load current determined for the un-faulted phase using (26) matches with the load current value determined using (25) is found.

An iterative process is used to determine the distance to the fault location from upstream switch:

- Select a line segment between bus *l* and (*l*+1), and let distance ratio, *d* varies between 0 and 1. The distance ratio is varied in incremental steps determined upon the desired accuracy.
- Using (26) the load current is determined corresponding to each phase for each value of *d*.
- For un-faulted phase, the current difference $I^{var} = \|I_L^{l(a)} - I_f^{l(a)}\|$ against *d*, is plotted for the entire length of the line segment. Using the plot, the minimal difference, $\min(I^{var})$ for the line segment is determined.
- If $\min(I^{var}) < \delta$, i.e., a fault current equals a load current, and minimum value does not correspond to the end of the line segment, then the distance to fault is the corresponding value of *d* multiplying by the line length.
- Otherwise, the fault is in one of the next line segments. The fault voltage and current are determined at the next bus (*l* + 1) as:

$$V_f^{l+1} = V_f^l - z_{ll}^l I_f^l \quad (28)$$

$$I_f^{l+1} = I_f^l - (z_L^{l+1})^{-1} V_f^{l+1} \quad (29)$$

- The above steps are repeated, until a first point on an un-faulty phase of the lateral where a fault current equals a load current is found.

2). Algorithm for locating three phase fault

Fig. 10 shows an example of a three phase fault at the line segment between buses *l* and (*l* + 1).

As shown in Fig. 10, ideally the fault impedances are resistances, or three phases balanced, then the imaginary parts of equivalent fault impedances at phase *a*, phase *b* and phase *c*

are equal to each other, that is $\text{imag}(Z_{F_a}) = \text{imag}(Z_{F_b}) = \text{imag}(Z_{F_c})$, where Z_{F_a} , Z_{F_b} and Z_{F_c} are the equivalent fault impedance at the fault location for phase *a*, phase *b* and phase *c* respectively.

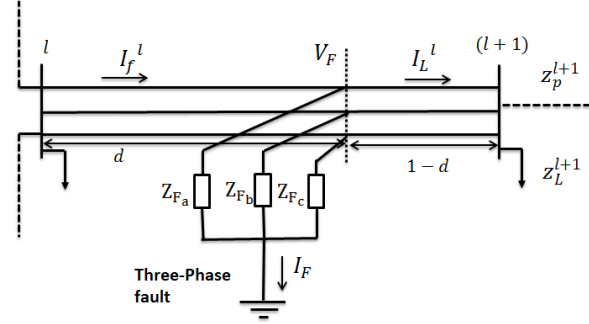


Fig. 10. A line segment with a three phase fault

Similar as double-phase faults, the locating of three-phase faults is also implemented sequentially for each line-segment. For each line segment, the load currents can be determined for each phase using (26), and the corresponding fault impedances can be determined using (22)-(24) by varying the ratio of distance to the fault over total line length, *d*. The estimated fault location is obtained when the value of the distance ratio, *d* that gives minimum difference in three phase reactance is found.

The steps for determining the distance to the fault location from upstream switch are listed below:

- Choose a line segment between buses *l* and (*l* + 1), and let the ratio of distance to the fault location over line length, *d* varies between 0 and 1.
- Using (26) calculate the load current corresponding to each phase for each value of *d*.
- Using (24) calculate the equivalent fault impedances, Z_{F_a} , Z_{F_b} and Z_{F_c} , and determine the difference between imaginary parts of equivalent fault impedances, X_F^{var} for a set of points with a different ratio *d* according to:

$$X_F^{var} = \left| \text{imag}(Z_{F_a}) - \text{imag}(Z_{F_b}) \right| + \left| \text{imag}(Z_{F_b}) - \text{imag}(Z_{F_c}) \right| + \left| \text{imag}(Z_{F_c}) - \text{imag}(Z_{F_a}) \right|$$

- Plot X_F^{var} verse *d* for the entire length of the line segment, and determine the minimal difference between imaginary parts, $\min(X_F^{var})$ for the line segment.
- If $\min(X_F^{var}) < \delta$, and minimum value does not correspond to the end of the line segment, then the fault is determined at a location corresponding to the ratio of distance to fault over total line length, *d*.
- Otherwise, the fault is in one of the next downstream line segments. The fault voltage and current at the next bus (*l* + 1) can be determined using (28), and (29).
- The above steps are repeated for each line segment, until a point with a difference between imaginary parts of

equivalent fault impedances at three phases below a threshold is found.

V. NUMERICAL EXAMPLES

The proposed method has been tested with several sample ungrounded systems, and satisfactory results are obtained.

Fig. 11 gives an example of test distribution systems. The system includes 1 three-phase transformer, and 3 feeders. Each feeder has 1 feeder breaker, 2 intelligent switches, 18 three-phase line segments, and 22 three-phase buses. All loads are DELTA-connected constant-PQ loads. Each line segment is a 1.25-mile long underground-cable, and the maximum length for each feeder is 15 miles. The self-impedances of the line segment at phase *a*, *b* and *c* are (0.4751+j0.2973), (0.4488+j0.2678), and (0.4751+j0.2973) ohms per mile respectively. The mutual impedances between phase *a* and phase *b*, phase *b* and phase *c*, and phase *c* and phase *a* are (0.1629-j0.0326), (0.1629-j0.0326), and (0.1234-j0.0607) ohms per mile. The self-susceptance of each phase is 127.8306 micro Siemens per mile.

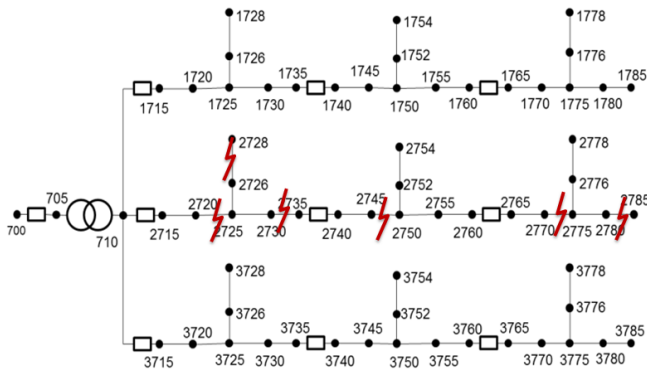


Fig. 11. A sample ungrounded distribution system

The tests are conducted with an Intel i5-2.40 GHz CPU. Both the feeder breakers and intelligent switches are measured with three-phase voltages, and three-phase currents.

Table I-IV list the test results for four different types of faults, and for each type of fault, six different fault locations are tested. The actual fault is located at a location with distance of 47.25% of the line length from the upstream terminal bus of the line segment. The incremental distance step used is 0.00312 miles.

TABLE I
TEST RESULTS ON DOUBLE-PHASE-TO-GROUND FAULTS

Fault Location	Line Location	Prediction Error(miles)	Prediction Error(%)	Computation Time(ms)
2720-2725	Mainline	0.00001	0.00004	1.713
2730-2735	Mainline	0.00001	0.00007	1.645
2745-2750	Mainline	0.00004	0.00025	1.527
2726-2728	Lateral	0.59063	3.9375	3.665
2752-2754	Lateral	0.59062	3.9375	3.675
2770-2775	Lateral	0.59062	3.9375	7.517
2780-2785	Lateral	0.59062	3.9375	7.540

The test results for double-phase faults are given in Table I and Table II. The fault types of Table I and Table II are double-phase-to-ground faults, and phase-to-phase faults respectively.

TABLE II
TEST RESULTS ON PHASE-TO-PHASE FAULTS

Fault Location	Line Location	Prediction Error(miles)	Prediction Error(%)	Computation Time(ms)
2720-2725	Mainline	0.00001	0.00008	1.725
2730-2735	Mainline	0.00002	0.00015	1.642
2745-2750	Mainline	0.00001	0.00005	1.539
2726-2728	Lateral	0.59063	3.9375	3.354
2752-2754	Lateral	0.59062	3.9375	3.610
2770-2775	Lateral	0.59062	3.9375	6.976
2780-2785	Lateral	0.59062	3.9375	7.455

The test results for three-phase faults are given in Table III and Table IV. Table III is for three-phase-to-ground faults, and Table IV is for phase-to-phase-to-phase faults.

TABLE III
TEST RESULTS ON THREE-PHASE-TO-GROUND FAULTS

Fault Location	Line Location	Prediction Error(miles)	Prediction Error(%)	Computation Time(ms)
2720-2725	Mainline	0.00001	0.00008	1.866
2730-2735	Mainline	0.00000	0.00001	1.640
2745-2750	Mainline	0.00000	0.00003	1.588
2726-2728	Lateral	0.00312	0.02083	3.464
2752-2754	Lateral	0.00312	0.02083	3.457
2770-2775	Lateral	0.00312	0.02083	7.337
2780-2785	Lateral	0.00312	0.02083	7.132

TABLE IV
TEST RESULTS ON PHASE-TO-PHASE TO-PHASE FAULTS

Fault Location	Line Location	Prediction Error(miles)	Prediction Error(%)	Computation Time(ms)
2720-2725	Mainline	0.00001	0.00008	2.093
2730-2735	Mainline	0.00001	0.00007	1.984
2745-2750	Mainline	0.00002	0.00015	1.579
2726-2728	Lateral	0.21563	1.43750	3.433
2752-2754	Lateral	0.46562	3.10417	3.225
2770-2775	Lateral	0.60312	4.02083	7.113
2780-2785	Lateral	0.76563	5.10417	7.048

As shown in the above tables, the proposed approach is capable of producing fault location prediction results very quickly. For the test cases on the mainline, it can predict the fault location very accurately within 1.866 milliseconds. For the test cases on the laterals, it can predict the fault location with maximum prediction error 5.1% in 7.540 milliseconds.

VI. CONCLUSIONS

This paper has proposed a novel impedance-based fault location algorithm for an ungrounded distribution system in event of a multi-phase faults.

The algorithm makes an efficient use of distribution circuit topology, and a set of one-ended and two-ended fault location algorithms are implemented to handle feeder section with different measuring and topology conditions.

Both one-ended and two-ended fault location algorithms proposed in this paper are novel in their approach and make no assumption regarding fault impedance.

The given test results have proven the effectiveness of proposed method.

REFERENCES

- [1] M. M. Saha, J. J. Izykowski, and E. Rosolowski, *Fault Location on Power Networks*, London : Springer-Verlag, 2010.
- [2] P. Verho, M. M. Saha, R. Das and D. Novosel, "Review of Fault Location Techniques for Distribution Systems", presented at *Power Systems and Communications Infrastructures for the future*, Beijing, September 2002.
- [3] D. Novosel, D. Hart, Y. Hu, and J. Myllymaki, "System for locating faults and estimating fault resistance in distribution networks with tapped loads", US Patent number 5,839,093, November 17, 1998.
- [4] R. Das, M.S. Sachdev and T.S. Sidhu, "A Fault Locator for Radial Sub-transmission and Distribution Lines", presented at *IEEE PES Summer Meeting*, Seattle, Washington, July 2000.
- [5] M. M. Saha, F. Provoost and E. Rosolowski, "Fault Location method for MV Cable Network", *DPSP*, Amsterdam, The Netherlands, pp. 323-326, April 2001.
- [6] R.H. Salim, M. Resener, A.D. Filomena, K. Rezende Caino de Oliveira, and A.S. Bretas, "Extended Fault-Location Formulation for Power Distribution Systems", *IEEE Transactions on Power Delivery*, vol.24, no.2, pp.508-516, April 2009.
- [7] D. Thomas, R. Carvalho and E. Pereira, "Fault Location in Distribution Systems Based On Traveling Wave", in *Proceedings of Power Technology Conference*, vol. 2, pp. 468-472, June 2003.
- [8] Z.Q. Bo, G. Waller and M. A. Redfern, "Accurate Fault Location Technique For Distribution System Using Fault-Generated High-Frequency Transient Voltage Signals", *IEE Proceedings on Generation, Transmission and Distribution*, vol. 146, no.1, pp. 73-79, January 1999.
- [9] Y. Tang, H.F. Wang, R.K. Aggarwal and A.T. Johns, "Fault Indicator in Transmission and Distribution Systems", in *Proceedings of Electric Utility Deregulation and Restructuring and Power Technologies*, London, UK, pp: 238-243, 2000.
- [10] H. Nouri, C. Wang, and T. Davies, "An accurate fault location technique for distribution lines with tapped loads using wavelet transform", in *IEEE Power Tech Proceedings*, Porto, Portugal, vol. 3, pp. 1-4, September 2001.
- [11] J. J. Mora, G. Carrillo, and L. Perez, "Fault location in power distribution systems using ANFIS Nets and current patterns", presented at *IEEE PES Transmission and Distribution Conference and Exposition, Latin America*, Caracas, Venezuela, 2006.
- [12] J. Mora-Florez, V. Barrera-Nuez, and G. Carrillo-Caicedo, "Fault location in power distribution Systems using a learning algorithm for multivariable data analysis", *IEEE Transactions on Power Delivery*, vol. 22, no. 3, pp. 1715-1721, July 2007.

Anamika Dubey received a M.S degree in Electrical and Computer Engineering from the University of Texas at Austin in 2012. She is a student member of IEEE. Currently, she is a Ph.D. student in the Department of Electrical and Computer Engineering at the University of Texas at Austin, USA. Her research interests include power system analysis and planning, power quality, grid reliability, and integration of smart grid technologies into distribution system.

Hongbo Sun received a Ph.D. degree in Electrical Engineering from Chongqing University, China in 1991. He is a senior member of IEEE. He is currently working at Mitsubishi Electric Research Laboratories in Cambridge,

Massachusetts, USA. His research interests include power system planning and analysis, power operation and control, and smart grid applications.

Daniel Nikovski received a Ph.D. degree in Robotics from Carnegie Mellon University in Pittsburgh, USA, in 2002. He is currently working at Mitsubishi Electric Research Laboratories in Cambridge, Massachusetts, USA. His research interests include machine learning, optimization and control, and numerical methods for analysis of complex industrial systems.

Jinyun Zhang received her Ph.D. in Electrical Engineering from the University of Ottawa, Canada in 1991. She is a fellow of IEEE. She is currently working at Mitsubishi Electric Research Laboratories in Cambridge, Massachusetts, USA. Her research interests include digital signal processing, wireless communications, optical networks, and smart grid applications.

Tomihiko Takano received M.S degree in precision engineering from Kyoto University in 1989. He is a senior member of IEEEJ, a member of SICE, CIGRE. He is currently working at the Advanced Technology R&D Center, Mitsubishi Electric Corp. His research interests include operation, control and protection for power systems, distribution resources, micro-grids.

Yasuhiro Kojima received a Ph.D. degree from Osaka University, Japan in 2008. He is a senior member of IEEEJ, a member of IEEE. He is currently working at the Advanced Technology R&D Center, Mitsubishi Electric Corp. His research interests include smart information technology applications for social infrastructure like power systems.

Tetsufumi Ohno received M.S degree in human information engineering from Osaka University in 2009. He is a member of IEEEJ. He is currently working at the Advanced Technology R&D Center, Mitsubishi Electric Corp. His research interests include distribution system analysis and control.